Published in Proc. of IEEE Intelligent Vehicles Symposium, 2012. DOI: http://dx.doi.org/10.1109/IVS.2012.6232299

Multipath Mitigation in GNSS-based Localization using Robust Optimization

Niko Sünderhauf, Marcus Obst, Gerd Wanielik and Peter Protzel

***Abstract*— Our paper adapts recent advances in the SLAM (Simultaneous Localization and Mapping) literature to the problem of multipath mitigation and proposes a novel approach to successfully localize a vehicle despite a significant number of multipath observations. We show that GNSS-based localization problems can be modelled as factor graphs and solved using efficient nonlinear least squares methods that exploit the sparsity inherent in the problem formulation. Using a recently developed novel approach for robust optimization, satellite observations that are subject to multipath errors can be successfully identified and rejected *during* the optimization process. We demonstrate the feasibility of the proposed approach on a real-world urban dataset and compare it to an existing method of multipath detection.**

I. INTRODUCTION

A common challenge for GNSS-based localization is the multipath problem that occurs for instance in urban areas with high buildings. Although the direct line of sight to a satellite is blocked by a building, its signal may still reach the receiver on the ground via one or several reflections on building structures or the ground. Since the signal path is longer for the reflected signal, ranging errors occur that can either prolongate the observed pseudorange or, due to correlation effects, shorten it. Multipath effects can also occur when the direct line of sight is free. In this situation, the signal is received directly, but is also reflected on a building or another structure in the vicinity of the receiver. Hence the signal is received multiple times, leading to correlation errors. The observations that are subject to multipath effects can be considered *outliers* that can severely bias the least squares estimate of the receiver's position. Even a single multipath measurement can lead to a defective position estimate. The problem gets worse if one considers that in urban environments not only one, but several satellite observations might be affected by multipath effects.

Our paper transfers recent advances in robust optimization from the field of SLAM (Simultaneous Localization and Mapping) in robotics to the domain of GNSS-based localization. In our recent work [1] [2] we addressed the problem of outliers in pose graph SLAM and developed a novel least squares formulation that is robust against such outliers. The approach proposed there is very versatile and can be applied to other least squares problems where outliers have to be expected. Therefore we can successfully transfer the gained insights from SLAM into the domain of GNSS-based localization.

All authors are with the Faculty of Electrical Engineering and Information Technology, Chemnitz University of Technology, 09111 Chemnitz, Germany niko.suenderhauf@etit.tu-chemnitz.de

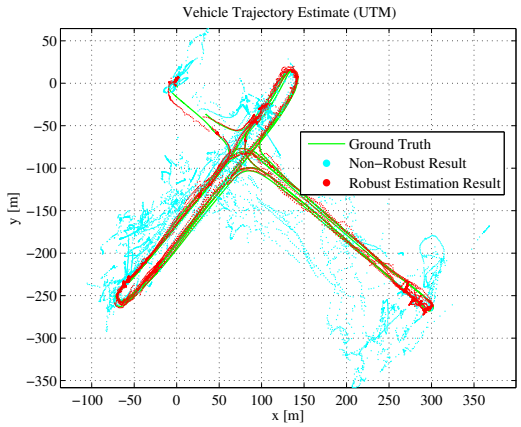

Fig. 1. Estimated vehicle trajectory in an urban scenario. While the conventional estimate (blue) based on the pseudorange readings from a consumer-class GPS receiver is extremely biased due to multipath errors, the robust estimation method proposed in this paper is able to detect and reject these outlier observations. The resulting trajectory estimate (red) is much closer to the ground truth (green).

Our paper demonstrates how multipath observations can be identified and rejected *during* the least squares optimization that solves for the position estimate, without additional a priori knowledge or additional sensor information. We provide an introduction to factor graphs and how the GNSS-based localization problem can be expressed using such a graph structure. This will help to understand the key idea of the proposed robust optimization scheme. Fig. 1 presents results acquired from a real-world dataset and compares our proposed solution against a highly accurate ground truth and a different method for multipath detection developed in related work.

II. MULTIPATH IDENTIFICATION AND MITIGATION – RELATED WORK

Different approaches for multipath mitigation are known to the literature, besides hardware-related approaches like using special antenna designs (e.g. choke ring) or antenna arrays. For instance [3] discusses the application of RAIM (Receiver Autonomous Integrity Monitoring) while [4] explores RANSAC-like algorithms. [5] proposes to actively determine occluded satellites with the help of an omnidirectional infrared camera mounted on the vehicle.

[6] and [7] propose to identify multipath observations by using information about the local building structure, i.e. a database of building positions and dimensions. Given an estimate on the receiver's position on the ground, raytracing

(a) (b)

Fig. 2. Two vehicle state nodes with their associated pseudorange factors (green). (a) in the most general graphical model, there are no connections between the vehicle state nodes. In (b), a state transition factor joins two successive vehicle nodes.

approaches can determine whether the direct line of sight to a received satellite is blocked by a building (and thus the signal was received via a reflection, causing multipath range errors). Clearly this method is well suited for multipath signal rejection, but requires considerable additional knowledge about the environment and a good initial guess of the receiver's position on the ground to perform the raytracing.

III. Factor Graphs

Factor graphs are bipartite undirected graphs and have been proposed by [8] as a general tool to model factorizations of large functions with many variables into smaller local subsets. The idea can be applied to probabilistic problems like SLAM or GNSS-based localization. The key idea is that a joint probability distribution can be expressed as a product over several single *factors* (of course adhering the conditional dependencies etc.), e.g.

$$P(X|U,Z) = \prod_i P(\mathbf{x}_i|\mathbf{u}_i,\mathbf{x}_{i-1}) \cdot \prod_{i,j} P(\mathbf{x}_i|\mathbf{z}_j) \quad (1)$$

where $\mathbf{x}_i$ are for instance the vehicle states, $\mathbf{u}_i$ are control inputs and $\mathbf{z}_j$ are measurements of any kind.

Factor graphs contain two types of nodes: one for variables and the other for the probabilistic constraints or factors. The edges in the graph therefore nicely capture the dependencies between the variables. In the context of GNSS-based localization, one type of nodes represents the unknown vehicle state variables $\mathbf{x}_i$, while the other type of node encodes the relations between them (e.g. via a state transition model) or the pseudorange measurements. Fig. 2 illustrates this concept.

IV. Modelling the GNSS-based Localization Problem as a Factor Graph

The least squares optimization problem that has to be solved when estimating the receiver position from a number of satellite observations can be easily modelled as a factor graph. In the most simple formulation, the vehicle position estimates are treated as conditionally independent. However, this notation can be extended by introducing motion models or other state transition relations.

Fig. 2 illustrates possible layouts of the factor graph for the GNSS-based localization problem. Remember that the large nodes represent the unknown variables, hence the sought state estimates and the small nodes represent the probabilistic factors that govern these variables. The vehicle state nodes and a few possible factors are explained in the following.

A. The Vehicle State Vertices

The state space contains at least the 3D position of the vehicle and the receiver clock error, leading to a state space that is at least 4-dimensional:

$$\mathbf{x} \in \mathbb{R}^4 = (x, y, z, \delta^{\text{clock}})^T \quad (2)$$

This state space may be extended by jointly estimating the vehicle orientation θ, velocity v, rotation rate ω or the clock error drift $\dot{\delta}^{\text{clock}}$, depending on the requirements and which other sensors are used. Estimating the vehicle acceleration a or road curvature $1/r$ would also be possible.

B. The Pseudorange Factor

A number of satellites are observed from every vehicle state $\mathbf{x}_t$, each providing a pseudorange measurement ρ_{tj}. Given the receiver position $\mathbf{x}_t^{x,y,z}$ and the position of the observed satellite $\mathbf{x}_{tj}^{\text{SAT}}$, the expected pseudorange measurement is given by the measurement function

$$h(\mathbf{x}_t, j) = \|\mathbf{x}_{tj}^{\text{SAT}} - \mathbf{x}_t^{x,y,z}\| + \delta^{\text{EarthRotation}} + \delta^{\text{Atmosphere}} + \mathbf{x}_t^{\delta^{\text{clock}}} \quad (3)$$

The terms $\delta^{\text{EarthRotation}}$ and $\delta^{\text{Atmosphere}}$ correct ranging effects caused by the earth's rotation and atmosphere (ionospheric and tropospheric propagation errors). $\delta^{\text{EarthRotation}}$ is given by

$$\delta^{\text{EarthRotation}} = \omega^{\text{Earth}} \frac{x_{tj}^{\text{SAT}} \cdot y_t - y_{tj}^{\text{SAT}} \cdot x_t}{c} \quad (4)$$

with ω^{Earth} the earth's rotation rate and c the speed of light.

If we assume the measured pseudorange ρ_{tj} is given by the measurement function $h(\mathbf{x}_t, j)$ plus a zero-mean Gaussian error term, thus

$$\rho_{tj} = h(\mathbf{x}_t, j) + \mathcal{N}(\mathbf{0}, \Sigma_{tj}) \quad (5)$$

then the error function of a single pseudorange factor is given as

$$\|\mathbf{e}_{tj}^{\text{pr}}\|^2_{\mathbf{\Sigma}_{tj}} = \|h(\mathbf{x}_t, j) - \rho_{tj}\|^2_{\mathbf{\Sigma}_{tj}} \quad (6)$$

with $\mathbf{\Sigma}_{tj}$ the covariance associated to the pseudorange measurement ρ_{tj}. Notice that minimizing above error over $\mathbf{x}_t$ corresponds to maximizing the likelihood function $L(\rho_{tj}|\mathbf{x}_t) \sim \mathcal{N}(h(\mathbf{x}_t, j), \mathbf{\Sigma}_{tj})$.

C. The State Transition Factor

Besides the obligatory pseudorange factors, additional factors can be modelled to incorporate more information or sensor data. A possible way to account for the receiver clock error is to model it as either constant over time, i.e. $\delta_{t+1}^{\text{Clock}} = \delta_t^{\text{Clock}} + \lambda$ where λ is a zero-mean Gaussian. Another possibility is to use a a constant drift model, i.e.

$$\delta_{t+1}^{\text{Clock}} = \delta_t^{\text{Clock}} + \dot{\delta}_t^{\text{Clock}} \Delta t + \mathcal{N}\left(0, \sigma_t^{\text{Clock}}\right) \quad (7)$$

$$\dot{\delta}_{t+1}^{\text{Clock}} = \dot{\delta}_t^{\text{Clock}} + \mathcal{N}\left(0, \sigma_t^{\text{ClockDrift}}\right) \quad (8)$$

For the latter case, the error function associated with the state transition factor is

$$\|\mathbf{e}_t^{\text{st}}\|^2_{\mathbf{\Sigma}_t^{\text{st}}} = \left\| \begin{pmatrix} \delta_t^{\text{Clock}} + \dot{\delta}_t^{\text{Clock}} \Delta t \\ \dot{\delta}_t^{\text{Clock}} \end{pmatrix} - \begin{pmatrix} \delta_{t+1}^{\text{Clock}} \\ \dot{\delta}_{t+1}^{\text{Clock}} \end{pmatrix} \right\|^2_{\mathbf{\Sigma}_t^{\text{st}}} \quad (9)$$

$\mathbf{\Sigma}_t^{\text{st}} = \text{diag}(\sigma_t^{\text{Clock}}, \sigma_t^{\text{ClockDrift}})$ is, as usual, the covariance matrix associated with the state transition factor at time t.

TABLE I
AVAILABLE OPTIMIZATION-BASED BACK-ENDS FOR SLAM.

Name	Main Publication	Source
g2o	[11]	`www.openslam.org`
MTK	[12]	`www.openslam.org`
gtsam	[10]	`collab.cc.gatech.edu/borg/gtsam`

D. Solving for the Maximum a Posteriori Solution

When only the pseudorange measurements are given, the maximum a posteriori solution for a single vehicle state $\mathbf{x}_t$ is found by solving the least squares problem

$$\mathbf{x}_t^* = \underset{\mathbf{x}_t}{\operatorname{argmin}} \sum_j \|\mathbf{e}_{tj}^{\text{pr}}\|^2_{\mathbf{\Sigma}_{tj}} \tag{10}$$

Similarly, we can solve for a set of vehicle states $X = \{\mathbf{x}_t\}$:

$$X^* = \underset{X}{\operatorname{argmin}} \sum_{tj} \|\mathbf{e}_{tj}^{\text{pr}}\|^2_{\mathbf{\Sigma}_{tj}} \tag{11}$$

Any additional factors that account for further measurements and sensor data can be easily incorporated by extending the error function. For instance to incorporate the state transition factors, we solve

$$X^* = \underset{X}{\operatorname{argmin}} \sum_{tj} \|\mathbf{e}_{tj}^{\text{pr}}\|^2_{\mathbf{\Sigma}_{tj}} + \|\mathbf{e}_{t}^{\text{st}}\|^2_{\mathbf{\Sigma}_{t}^{\text{st}}} \tag{12}$$

and so forth. Notice that it is very easy to incorporate more factors, e.g. a motion model or additional inter-vehicle information.

In its general structure, the GNSS-based least squares localization problem is not different to any of the problems encountered when solving the SLAM problem in robotics. The important insight to why the above optimization problem is solvable efficiently lies in its sparse structure. That is, a variable $\mathbf{x}_t$ is only dependent on a few other variables or observations. The recent SLAM literature [9]–[11], has developed a number of approaches that exploit this sparse structure and lead to highly efficient problem solvers. These solvers and frameworks are available to the community and can almost immediately be applied to the domain of GNSS-based localization. Table I lists the most recent and important developments.

V. TOWARDS A PROBLEM FORMULATION ROBUST TO MULTIPATH ERRORS

If multipath observations occur, some of the pseudorange observations are *outliers* to our least squares optimization problem. It is generally known that least squares methods are by default not robust against such outliers and that even a single outlier can have catastrophic effects on the estimation result.

Our main idea to increase the robustness of the optimization is that the topology of the factor graph representation should be subject to the optimization instead of keeping it fixed. This is achieved by introducing another type of hidden variable into the problem formulation: A *switch variable* s_{tj} is associated with each factor that could potentially represent an outlier. The optimization now works on an augmented problem, searching for the joint optimal configuration of the original variables and the newly introduced switch variables, hence searching the optimal graph topology. These ideas were developed in the context of SLAM in [1] and [2]. We describe their application to the GNSS-based localization problem in the following.

A. The Switched Pseudorange Factor

By combining the pseudorange factor from section IV-B with the newly introduced switch variables, we gain the *switched* pseudorange factor:

$$\|\mathbf{e}_{tj}^{\text{spr}}\|^2_{\mathbf{\Sigma}_{tj}} = \|\Psi(s_{tj}) \cdot (h(\mathbf{x}, j) - \rho_{tj})\|^2_{\mathbf{\Sigma}_{tj}} \tag{13}$$

The function Ψ is called the *switch function*. This switch function is defined as $\Phi : \mathbb{R} \to [0, 1]$, i.e. it is a mapping from the continuous real numbers to the interval $[0, 1]$, defined on $\mathbb{R}$. Different switch functions can be defined, e.g. a step function, or a sigmoid. However, our experiments in earlier work showed that a simple linear function of the form

$$\omega_{tj} = \Psi_a^{\text{lin}}(s_{tj}) : \mathbb{R} \to [0, 1] = \begin{cases} 0 & : s_{tj} < 0 \\ \frac{1}{a} s_{tj} & : 0 \leq s_{tj} \leq a \\ 1 & : s_{tj} > a \end{cases} \tag{14}$$

with parameter $a = 1$ is a suitable choice.

The idea behind the switch variables is that the influence of a pseudorange measurement can be removed by driving the associated switch variable s_{tj} to a value so that $\omega_{tj} = \Phi(s_{tj}) \approx 0$. Notice that it is not possible to use the weights ω_{tj} directly as variables in the optimization, since they are only defined on the interval $[0, 1]$, which is not suitable to the applied least squares optimization approaches that require continuous domains.

The influence of the switch variables can be described and understood in two equivalent ways: In the topological interpretation, a switch can enable or disable the constraint edge it is associated with, thus literally remove it from the graph topology. In the probabilistic interpretation, the switch variable influences the information matrix of the factor it is associated with and can drive it from its original value to zero, thus increasing the covariance associated with this factor until infinity. It has been shown that both interpretations are equivalent [2].

To prevent the optimization from simply rejecting all pseudorange observations, an additional *switch prior* factor is needed that anchors each switch variable s_{tj} at its initial value γ_{tj}. It is defined as:

$$\|\mathbf{e}_{tj}^{\text{sp}}\|^2_{\mathbf{\Xi}_{tj}} = \|s_{tj} - \gamma_{tj}\|^2_{\mathbf{\Xi}_{tj}} \tag{15}$$

Combining these two factors leads to the extended robust problem formulation:

$$X^* = \underset{X}{\operatorname{argmin}} \sum_{tj} \|\mathbf{e}_{tj}^{\text{spr}}\|^2_{\mathbf{\Sigma}_{tj}} + \|\mathbf{e}_{tj}^{\text{sp}}\|^2_{\mathbf{\Xi}_{tj}} \tag{16}$$

Fig. 3 illustrates this extended formulation for a single vehicle state variable. Notice how each pseudorange measurement is associated with its own switch variable.

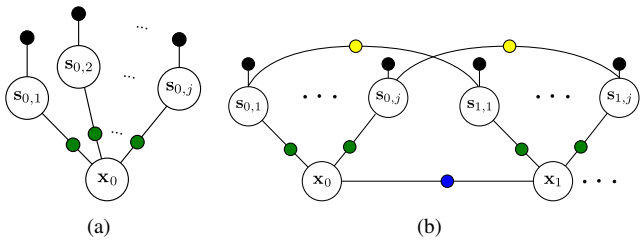

Fig. 3. (a) A vehicle state vertex with three switched pseudorange factors $\mathbf{e}^{\text{spr}}$ (green), the associated switch variables and their prior factors $\mathbf{e}^{\text{sp}}$ (black). (b) Illustration of the most complex factor graph used in this paper: The switch variables are connected by switch transition factors $\mathbf{e}^{\text{swt}}$ (yellow) and the state transition factors $\mathbf{e}^{\text{st}}$ (blue) connect the state vertices.

B. The Switch Transition Factor

In contrast to the switch variables in the pose graph SLAM problem, the switch variables in the GNSS-based localization problem are not independent: If a satellite j is observed from two successive vehicle locations $\mathbf{x}_{t-1}$ and $\mathbf{x}_t$, then s_{tj} is likely to be equal to $s_{t-1,j}$. We can capture this conditional dependence and model $P(s_{ij}|s_{t-1,j})$ as a Gaussian with

$$P(s_{tj}|s_{t-1,j}) \sim \mathcal{N}\left(s_{t-1,j}, \mathbf{\Sigma}_{tj}^{\text{swt}}\right) \tag{17}$$

which leads us to the *switch transition* factor

$$\|\mathbf{e}_{tj}^{\text{swt}}\|_{\mathbf{\Sigma}_{tj}^{\text{swt}}}^2 = \|s_{tj} - s_{t-1,j}\|_{\mathbf{\Sigma}_{tj}^{\text{swt}}}^2 \tag{18}$$

that can be easily incorporated as an additional factor into the overall optimization problem. Using the switch transition factors, we would solve

$$X^* = \underset{X}{\operatorname{argmin}} \sum_{tj} \|\mathbf{e}_{tj}^{\text{spr}}\|_{\mathbf{\Sigma}_{tj}}^2 + \|\mathbf{e}_{tj}^{\text{sp}}\|_{\mathbf{\Xi}_{tj}}^2 + \|\mathbf{e}_{tj}^{\text{swt}}\|_{\mathbf{\Sigma}_{tj}^{\text{swt}}}^2 \tag{19}$$

for the maximum a posteriori estimate of X. More factors (e.g. a motion model) can be incorporated in the same convenient way.

VI. Multipath Mitigation in a Real-World Urban Scenario

While the previous section explained the different factors necessary for multipath mitigation, the approach is now evaluated using data collected in a real-world urban scenario. We will see how the raw GPS pseudoranges are affected by multipath effects supposedly caused by the tall buildings next to the area where the data was collected. The evaluation will show that the proposed scheme for robust optimization is able to mitigate these effects and decrease the overall estimation errors.

A. The Chemnitz City Dataset

The necessary data for the evaluation was collected in the city center of Chemnitz, Germany, using the Carai concept vehicle [13]. The vehicle was driven over a road junction several times. Fig. 4 visualizes the road layout, the ground truth trajectory, and the tall buildings nearby that caused a high number of GPS signal occlusions and reflections.

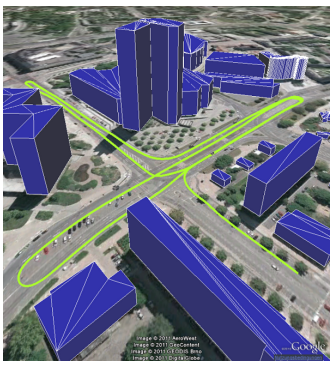

Fig. 4. Overview of the urban scenario used in the evaluation. The ground truth path of the vehicle is marked in green. Notice the tall buildings close to the streets. Image courtesy of Sven Bauer, [6].

TABLE II
Collected sensor information used for the evaluation.

Data	Sensor
GPS pseudoranges	consumer-class GPS receiver (ublox LEA4)
SBAS correction data	using EGNOS
ground truth trajectory	NovAtel OEM V DGPS with RTK and IMU

Among other sensor systems, the Carai vehicle is equipped with a high-precision differential GPS and inertial measurement unit that allows to determine the vehicle's position with a precision of 2 cm [14]. The position estimates of this high-precision unit were used as ground truth for the following analysis. In addition to the high-precision GPS unit, a consumer-class device (ublox LEA4) provided the pseudorange measurements that served as inputs for the optimization framework. Table II summarizes the collected sensor information.

B. Methodology

Given the collected data, we applied batch least squares optimization to solve for the maximum a posteriori estimate of the vehicle trajectory. That is, we estimated $X^* = \operatorname{argmax}_X P(X|Z)$ where $X = \{\mathbf{x}_{1:T}\}$ is the set of all vehicle states and $Z = \{\mathbf{z}_{1:T}\}$ is the set of all available sensor data (pseudorange observations). We constructed five different problem representations, using different combinations of the factors described in the previous section. Four of these five representations contained the switched pseudorange factors and thus are supposed to be robust or at least more robust against multipath errors than the conventional optimization approach. The optimization problems represented by the constructed factor graphs were solved using the C++ framework g^{2}o [11], after the different factors described above were implemented for this framework.

To compare the estimation results with the ground truth provided by the high-precision GPS and IMU-devices from the Carai vehicle, the RMSE metric was used. Notice that it only operated on the x and y component of the position estimates, given in the UTM coordinate frame, thus the metric is denoted RMSE_{xy}.

TABLE III

PARAMETERS USED IN THE EVALUATION.

Parameter	Value	Description
Ψ	Ψ_1^{lin}	switch function
γ_{tj}	1.0	switch prior value
$\mathbf{\Xi}_{tj}$	1.0	switch prior covariance
$\mathbf{\Sigma}_{tj}$	$(10\text{m})^2$	cov. of pseudorange measurements
$\mathbf{\Sigma}_{tj}^{\text{swt}}$	0.05^2	switch transition covariance
$\mathbf{\Sigma}_{tj}^{\text{st}}$	$\text{diag}(0.001\text{s}, 0.25\frac{\text{s}}{\text{s}})^2$	state transition covariance

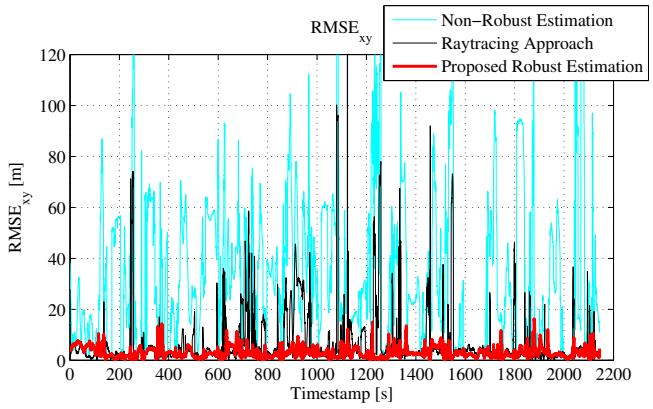

Fig. 5. RMSE metric compared for the proposed robust optimization (red), the conventional least squares (blue) and the raytracing method of [6] and [7] (black). Notice that the errors of the proposed robust optimization are constantly low while the other two approaches show significant spikes where the position estimation failed due to unhandled multipath effects.

Furthermore, we compare the solution of the robust optimization against a raytracing approach for multipath detection [6] [7].

C. Used Parameters

Table III lists the different parameters that were used in the implementation. The values in the upper part of the table correspond to the same parameters of the robust back-end we encountered in the SLAM context. They were chosen to have the same values as in our earlier work, which underlines that the proposed approach is generic and domain-independent. The values for the parameters in the lower part of the Table III are problem specific and were chosen empirically.

VII. RESULTS

The five different factor graph representations, the gained results in terms of RMSE and the required time until convergence on a Core2Duo desktop PC running at 2.4 GHz are summarized in Table IV. The first line of the table corresponds to the non-robust, conventional least squares solution, using only the pseudorange factors $\mathbf{e}^{\text{pr}}$. Due to a several multipath effects, reflections and occlusions, the RMSE values are very high, with a median error of over 25m.

When the conventional least squares pseudorange factors $\mathbf{e}^{\text{pr}}$ are replaced by their switched counterparts $\mathbf{e}^{\text{spr}}$, the quality of the estimation increases significantly. The next four

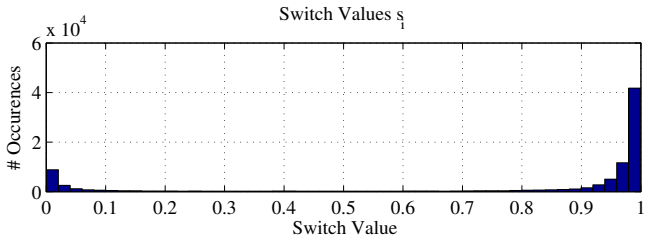

Fig. 6. Histogram over the switch values s_{tj} after the optimization for the best factor graph representation (using $\mathbf{e}^{\text{spr}}$, $\mathbf{e}^{\text{sp}}$, $\mathbf{e}^{\text{swt}}$, and $\mathbf{e}^{\text{st}}$). Notice that most switch variables are either approximately 1 or 0, but hardly any intermediate values exist. This means that the optimizer very clearly "decided" whether a satellite observation should be considered an outlier or an inlier. Using a splitting threshold of 0.5, 19165 of 90314 observations or roughly 21% have been declared an outlier.

lines in Table IV list the results of the different combinations of the proposes switched pseudorange factors with the state transition $\mathbf{e}^{\text{st}}$ and switch transition factors $\mathbf{e}^{\text{swt}}$.

The best results are achieved when combining all three proposed factors $\mathbf{e}^{\text{spr}}$, $\mathbf{e}^{\text{swt}}$, and $\mathbf{e}^{\text{st}}$ (marked red in Table IV). Using this problem formulation results in a median RMSE of only 2.45m and also the maximum error is reduced to 16.31m. The trajectory estimated with the combination of all three factors can be compared against the ground truth solution and the conventional, non-robust least squares solution in Fig. 1. These results are remarkable, especially if we compare them against the results gained by the raytracing approach to multipath detection [6] [7] in the last line of Table IV. Despite the large amount of additional information about the environment that was used in the raytracing method to decide whether satellites are visible from a certain point on the ground, the results of the proposed robust optimization reach better results. This also visible from Fig. 5 that shows the RMSE for each vehicle pose for the proposed robust estimation, the conventional least squares method and the raytracing approach of [6] and [7].

Fig. 6 illustrates the distribution of the individual switch values s_{ti} after the optimization. It is apparent that most switch variables have been assigned values of approximately 0 or 1. This supports the understanding that the optimization could clearly recognize the outlier measurements (multipath observations) and distinguish them from the inliers ("good" observations).

Tracking the values of the switch variables over time results in further interesting insights: Fig. 7 illustrates how some of the switch variables associated with a specific satellite evolve through time. The variables associated to different satellites are shown in different colors, so it is possible to see how the observations of a satellite are estimated to be outliers (thus subject to multipath effects) at one point in time and inliers later on. The switch values for most satellites oscillate between 1 and 0 as the satellite may be occluded by a building at one point in time, but clearly visible at another and so forth. The same behaviour was observed when not using state transition factors, thus only

TABLE IV

RMSE_{XY} VALUES AND CONVERGENCE TIME FOR DIFFERENT TRIALS ON THE CHEMNITZ CITY DATASET.

Method	Used Factors	Median [m]	Mean [m]	Max [m]	Time [s]
non-robust optimization	$\mathbf{e}^{\mathrm{pr}}$	25.28	32.85	171.64	1.2
robust optimization	$\mathbf{e}^{\mathrm{spr}}$, $\mathbf{e}^{\mathrm{sp}}$	3.66	17.91	171.61	84.3
	$\mathbf{e}^{\mathrm{spr}}$, $\mathbf{e}^{\mathrm{sp}}$, $\mathbf{e}^{\mathrm{st}}$	2.79	14.08	274.49	102.8
	$\mathbf{e}^{\mathrm{spr}}$, $\mathbf{e}^{\mathrm{sp}}$, $\mathbf{e}^{\mathrm{swt}}$	2.69	8.10	128.55	46.2
	$\mathbf{e}^{\mathrm{spr}}$, $\mathbf{e}^{\mathrm{sp}}$, $\mathbf{e}^{\mathrm{swt}}$, $\mathbf{e}^{\mathrm{st}}$	2.45	2.96	16.31	66.9
raytracing approach [6] [7]	N/A	2.92	6.83	509.12	665

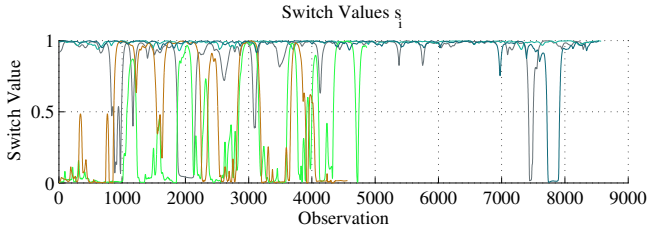

Fig. 7. The switch values associated to the pseudorange observations of a few observed satellites change over time as the observations are estimated to be inliers or outliers. A low switch value indicates the optimizer estimated the observation to be an outlier, i.e. subject to multipath effects. The switch values associated to different satellites are plotted in different colors.

the switched pseudorange factors and the switch transition factors. The behaviour without the switch transition appeared less coherent, which would be expected.

VIII. CONCLUSIONS

Our proposed robust optimization approach is able to detect and reject multipath measurements during the optimization process. It does not require an additional pre-processing step or additional knowledge or models of the environmental structure or the surrounding buildings. It outperforms the conventional non-robust least squares solution but also a sophisticated and computationally involved raytracing approach for multipath detection.

The proposed approach was ported from the author's earlier work [1] [2] in the domain of SLAM. A key difference to the SLAM problem however is that GNSS-based localization is usually understood as an *online* problem, i.e. it has to be solved while new measurements and observations arrive. In SLAM, we are sometimes satisfied with an *offline* or *batch* solution, after all the data has been gathered. However, since efficient methods for incremental optimization-based smoothing are available in the SLAM community (especially iSAM and iSAM2 [10]), we can solve the GNSS-based localization problem online in an incremental manner if it is required and still keep the factor graph representation to apply the robust approach that we proposed here. The most important future work therefore is to apply and evaluate the proposed robust optimization scheme in an *incremental*, sliding window mode, instead of performing batch processing as was performed in this paper. The incorporation of additional factors is worthwhile as well. Especially a motion model factor, using an a priori known map or inter-vehicle information for cooperative localization can significantly improve the estimation results.

REFERENCES

[1] N. Sünderhauf and P. Protzel, "BRIEF-Gist – Closing the Loop by Simple Means," in *Proc. of IEEE Intl. Conf. on Intelligent Robots and Systems (IROS)*, 2011.

[2] N. Sünderhauf and P. Protzel, "Towards a Robust Back-End for Pose Graph SLAM," in *Proc. of IEEE Intl. Conf. on Robotics and Automation (ICRA)*, 2012.

[3] Z. Qiang, Z. Xiaolin, and C. Xiaoming, "Research on RAIM Algorithm under the Assumption of Simultaneous Multiple Satellites Failure," in *Proc. of ACIS Intl. Conf. on Software Engineering, Artificial Intelligence, Networking, and Parallel/Distributed Computing*, 2007.

[4] X. Tu, D. Gu, D. Yi, and H. Zhou, "Evaluation of GNSS Receiver Autonomous Integrity Monitoring for multiple outliers with a smart random sample consensus strategy," in *Proc. of 19th International Conference on Geoinformatics*, 2011.

[5] J.-i. Meguro, T. Murata, J.-i. Takiguchi, Y. Amano, and T. Hashizume, "GPS Multipath Mitigation for Urban Area Using Omnidirectional Infrared Camera," *IEEE Transactions on Intelligent Transportation Systems*, vol. 10, no. 1, pp. 22 –30, march 2009.

[6] S. Bauer, M. Obst, and G. Wanielik, "3D Environment Modelling for GPS Multipath Detection in Urban Areas," in *9th International Multi-Conference on Systems, Signals and Devices*, 2012.

[7] M. Obst, S. Bauer, and G. Wanielik, "Urban Multipath Detection and Mitigation with Dynamic 3DMaps for Reliable Land Vehicle Localization," in *IEEE/ION PLANS*, 2012.

[8] F. Kschischang, B. Frey, and H.-A. Loeliger, "Factor graphs and the sum-product algorithm," *IEEE Transactions on Information Theory*, vol. 47, no. 2, pp. 498–519, Feb. 2001.

[9] K. Konolige, J. Bowman, J. D. Chen, P. Mihelich, M. Calonder, V. Lepetit, and P. Fua, "View-based maps," *International Journal of Robotics Research (IJRR)*, vol. 29, no. 10, 2010.

[10] M. Kaess, H. Johannsson, R. Roberts, V. Ila, J. Leonard, and F. Dellaert, "iSAM2: Incremental smoothing and mapping with fluid relinearization and incremental variable reordering," in *IEEE Intl. Conf. on Robotics and Automation, ICRA*, 2011.

[11] R. Kümmerle, G. Grisetti, H. Strasdat, K. Konolige, and W. Burgard, "g2o: A general framework for graph optimization," in *Proc. of the IEEE Int. Conf. on Robotics and Automation (ICRA)*, 2011. [Online]. Available: http://ais.informatik.uni-freiburg.de/publications/papers/kuemmerle11icra.pdf

[12] R. Wagner, O. Birbach, and U. Frese, "Rapid Development of Manifold-Based Graph Optimization Systems for Multi-Sensor Calibration and SLAM," in *Proc. of IEEE/RSJ Intl. Conf. on Intelligent Robots and Systems (IROS)*, 2011.

[13] R. Schubert, E. Richter, N. Mattern, P. Lindner, and G. Wanielik, "A concept vehicle for rapid prototyping of advanced driver assistance systems," in *Advanced Microsystems for Automotive Applications 2010*. Springer, 2010, pp. 211–219.

[14] S. Bauer, "Modellierung von GPS-Mehrwegeausbreitungen mit Hilfe von digitalen Karten und 3D-Modellen (Diplomarbeit)," Master's thesis, Hochschule für Technik und Wirtschaft, Dresden, Germany, 2011.